THE ASTROPHYSICAL JOURNAL, 393:L51–L54, 1992 July 10

HIGH-ENERGY SPECTRAL BREAKS IN GAMMA-RAY BURSTS

BRADLEY E. SCHAEFER, BONNARD J. TEEGARDEN, AND THOMAS L. CLINE
NASA/Goddard Space Flight Center, Code 661, Greenbelt, MD 20771
GERALD J. FISHMAN, CHARLES A. MEEGAN, ROBERT B. WILSON,
WILLIAM S. PACIESAS, AND GEOFFREY N. PENDLETON
NASA/Marshall Space Flight Center, ES-62, Huntsville, AL 35812
JAMES L. MATTESON AND DAVID L. BAND
University of California at San Diego, CASS-0111, La Jolla, CA 92093
AND
JOHN P. LESTRADE
Mississippi State University, P.O. Box 5167, Mississippi State, MS 39762
Received 1992 March 16; accepted 1992 April 22

ABSTRACT

We present model fits for 18 gamma-ray burst spectra from 100 keV to 27 MeV made with the BATSE spectroscopy detectors on the *Compton Gamma Ray Observatory*. Most of the bursts are well fitted as power laws with spectral indices between -1.36 and -2.29; however, five bursts show definite departures from a simple power-law fit at high energies. Three of these bursts are well fitted with broken power-law spectra and break energies of from 400 to 690 keV, such as might arise from photon-photon interactions. If so, then the source compactness and hence distance will be sharply constrained. Two of the bursts have spectra with sharply confined slope changes and are well fitted with broken power-law spectra with break energies of 1.2 and 1.6 MeV at peak, such as might arise from photon–magnetic field interactions. If so, then these spectral breaks provide strong evidence for the existence of high magnetic fields in the burst emission region.

Subject headings: gamma rays: bursts

1. INTRODUCTION

Several physical processes can result in breaks in the spectrum of a gamma-ray burst around 1 MeV. A spectral break occurs where the slope of the continuum has a sharp change over a small energy range. Generally, these breaks are caused by photon degradation processes that have some threshold at the break energy.

One such process is the photon-photon interaction, in which high-energy photons convert to electron-positron pairs, thus steepening the high-energy photon spectrum. The break energy should be at 511 keV with relativistic shifts due to beaming or high gravitational fields. The size of the spectral break depends on the source compactness.

Another process is the interaction of a single photon with a strong magnetic field, where high-energy photons passing through a magnetic field stronger than roughly 10^{12} G will likely produce electron-positron pairs and thus be lost to the observed spectrum. Baring (1990) has shown that the spectrum will appear as a broken power law. The break energy and magnitude will depend on the field strength and the particle distribution.

Another process that results in a spectral break is when repeated Compton scattering by power-law electrons degrades the high-energy photons. The steady state distribution will have a break at 511 keV or below due to the relativistic cutoff in the Klein-Nishina cross section (Zdziarski & Lamb 1986; Zdziarski 1987).

The degradation process can be identified by the statistics of the observed break energies. For photon-photon, photon–magnetic field, and repeated Compton interactions, the break energies will be >511 keV, >1 MeV, and <511 keV, respectively. Additional consistency tests for the photon-magnetic process can be made if a burst displays both cyclotron lines and high-energy breaks.

Much definite information about physical conditions in the emission region can be derived from the spectral breaks for each of the possible processes. Depending on the identity of the process, we can learn the beaming factor, source compactness, gravitational redshift, magnetic field strength, particle energy distribution, maximum pitch angle for the particles, or source optical depth (Schmidt 1978; Baring 1990).

Most gamma-ray burst detectors have not had the sensitivity required to obtain quality spectra to sufficiently high energy that spectral breaks could be detected. The best known exception is the gamma-ray spectrometer experiment on the *Solar Maximum Mission* (*SMM*) satellite, which has measured spectra up to 100 MeV (Share et al. 1986). Most *SMM* spectra are well fitted by a power law over the entire range of available data (from 300 keV to typically 10 MeV), although some fraction have a steepening of the spectra at high energies (Nolan et al. 1984). Some *SMM* spectra appear to show a broken power law with breaks near 2 MeV (Share et al. 1982, 1986; see also Zdziarski 1987). Furthermore, one burst seen with the SIGNE 2 MP9 experiment appears to have breaks near 500 keV (Kuznetsov et al. 1986). The Burst and Transient Source Experiment (BATSE) on the *Compton Gamma Ray Observatory* (launched 1991 April 5) has measured the spectra of many bursts to energies well above 1 MeV, so that this data base can be used to search for high-energy spectral breaks.

2. DATA AND ANALYSIS

BATSE consists of eight modules each containing two types of detectors; the large-area detectors (2025 cm^2 surface area

and 1.27 cm thick) and the spectroscopy detectors (SDs; 127 cm^2 surface area and 7.6 cm thick). This paper reports on SD data.

In the absence of a burst trigger, high-energy resolution spectra (256 pseudo-logarithmically spaced channels) are routinely accumulated for each SD with time resolution ranging from 60 to 300 s. These are typically used for background estimation in the burst analysis. When the on-board burst mode is triggered, 192 high-energy resolution spectra are accumulated into the trigger memory, with typical time resolution of from 0.128 to 1 s depending on the brightness history of the burst.

The energy range varies with the detector gain, with nominal gains of 0.4×, 1×, 4×, and 7× being used for individual detectors at various times. The associated energy ranges for valid data are roughly 150–27,000, 60–11,000, 15–2700, and 10–1600 keV, respectively. After 1991 July 29, the detectors with 0.4× gain (detectors 3 and 4) were changed to high gain (4× or 7×) in order to optimize the detection of cyclotron lines. Thus, after this change, our search for high-energy breaks usually used only detectors 2 and 5, which were at 1× gain.

In general, our search for high-energy breaks was restricted to energies greater than 100 keV. However, the SDs still have some residual calibration uncertainty at low energies relating to electronic nonlinearities. Thus, for 0.4× gain detectors, a lower energy limit of 300 keV was used in order to avoid completely any uncertainties in calibration. Moreover, the SDs also detect gamma rays from bursts which scattered off the Earth's atmosphere and were downgraded in energy, affecting the spectrum primarily in the 50–200 keV range. Since atmospheric scattering corrections have not yet been implemented in the spectral analysis software, we avoid this problem by restricting model fits to energies above 300 keV for any detector that points within 90° of the Earth's center.

We have selected the 18 brightest bursts at 1 MeV. The BATSE trigger number and the burst identification (YYMMDD-SSSSS of the trigger time) appear in columns (1) and (2) of Table 1. In general, we have extracted a count spectrum for each burst for the entire duration of the burst. Some bright bursts were examined over smaller time intervals. The choices of detectors for each burst (see col. [3] of Table 1) were made on the basis of gain (that is, low-gain detectors were used whenever possible) and the direction to the burst (a detector was used only if the burst was in the hemisphere of visibility). We have tried many alternative choices of detectors for model fitting, with no significant changes in the model fit parameters. The time intervals (in seconds since trigger time) for each spectrum examined, along with a brief description of the time interval, are given in columns (5) and (6) of Table 1.

The spectra for each burst, detector, and time interval were extracted and dead time corrected by standard techniques (Schaefer et al. 1991; Schaefer 1991). The background spectra were estimated on a channel-by-channel basis with a fit (a Taylor series with four terms) to nearby background spectra. The nontriggered background data always included from seven to 12 spectra from background data types with 60–300 s integrations ranging within half an hour of the trigger time. For about half the bursts the trigger memory data could be used to derive additional background spectra with better time resolution (typically 1 s durations) immediately after the burst. Ultimately, the model fit parameters were found to be relatively insensitive to the time intervals and fit constraints used for the background estimation.

As a test of the background generation, we have computed the background from nontrigger data and subtracted it from trigger memory data accumulated after the burst was clearly over. The resulting spectra are zero with a typical error of 5% of the background flux at all energies. At high energies, the statistical noise will dominate this systematic uncertainty. Nevertheless, we have tried restricting our fit to energy ranges over which the burst flux is greater than 10% of the background flux, with no significant difference in the results.

At high energies, the total number of background counts in each bin will be small for integration times of a few seconds or shorter. To keep the statistics of the counts in each bin close to a Gaussian (instead of Poisson) distribution, we have binned the count spectra before any model fits. The resulting binning typically has channels that are several times wider than the detector resolution. The total number of binned channels (N_{ch}) for each spectrum used for model fits is given in column (4). We have tried wide variations in our binning procedures, but find no significant difference in our results.

We have fitted each spectrum in Table 1 with three models. The models are a simple power law, an optically thin thermal bremsstrahlung with a constant Gaunt factor (OTTB), and a sharply broken power law. The model fitting and photon spectrum generation procedure is the traditional forward fitting method (Loredo & Epstein 1989; Schaefer 1991). Uncertainties in model fit parameters are found as in Lampton, Margon, & Bowyer (1976).

The χ^2 and fit parameters (other than the normalization constant) for each model for each spectrum are presented in Table 1. The α-value for the power-law model is the slope of the best-fit power law, where $\alpha = -2$ for a spectrum that has equal power for every decade of energy. The kT value is the characteristic energy (in keV) for an OTTB model by which the spectrum falls off exponentially with energy. The broken power-law model consists of a simple power law with index α_{low} below some break energy (E_{break} in keV), and a simple power law with index α_{high} above that break energy. The quoted χ^2 values have not been reduced by the number of degrees of freedom. The number of degrees of freedom is $N_{ch} - 2$ for the power law and OTTB models and $N_{ch} - 4$ for the broken power-law model.

The χ^2 statistics can be used to judge the relative quality of each model for each spectrum. We have followed the F-test as prescribed by Briggs (1991) for judging whether a spectrum shows significant curvature.

3. RESULTS

Roughly three-quarters of the bursts are consistent with the power-law model (see Fig. 1 for two examples). Ten of the 18 bursts are consistent with the OTTB model. All bursts are consistent with the broken power-law model. Three bursts (910430-61721, 910601-69736, and 910814-41082) show definite curvature, although these are well fitted by either OTTB or broken power-law models (see Fig. 1). Two bursts (910503-25454 and 910814-69275) show definite curvature which is poorly fitted by an OTTB model (see Fig. 1).

The uncertainties in the parameters for the broken power-law model will be the smallest for those spectra with the most clearly defined breaks. For the 0–14 s spectrum of burst 910503-25454, the 1 σ errors on the break energy, α_{low}, and α_{high} are 200 keV, 0.07, and 0.11. For the 0–4 s spectrum of burst 910814-69275, the errors are 110 keV, 0.03, and 0.19, respectively.

TABLE 1

DESCRIPTION OF SPECTRAL AND MODEL FIT RESULTS

Trigger Number (1)	Burst Identification (2)	Detectors (3)	N_{ch} (4)	Time Range (5)	Description of Interval (6)	Power Law χ^2 (7)	Power Law α (8)	OTTB χ^2 (9)	OTTB kT (10)	Broken Power Law χ^2 (11)	Broken Power Law E_{break} (12)	Broken Power Law α_{low} (13)	Broken Power Law α_{high} (14)
109	910425-02267	4,[a] 0,[b] 5[b]	90	0–39	All	194	−1.55	456	1130	193	2900	−1.57	−1.48
130	910430-61721	6,[b] 7[b]	49	0–40	All	95	−2.06	61	280	64	430	−1.82	−3.05
				0–15	Peak 1	85	−2.00	56	300	55	390	−1.65	−3.19
				15–23	Peak 2	48	−2.14	37	260	37	660	−1.86	−6[c]
				30–40	Peak 4	57	−2.15	49	260	46	680	−1.87	−6[c]
142	910502-81445	0,[a] 1,[b] 2[b]	75	0–39	All	1250	−1.39	5606	17500	1176	300[c]	−1.91	−1.27
143	910503-25454	4[a]	32	0–14	All[d]	64	−2.24	112	780	26	1040	−1.98	−2.58
				0–1.8	Peak 1	61	−2.05	63	1230	36	1190	−1.70	−2.42
				1.8–3.2	Peak 2	39	−2.10	60	1120	25	1220	−1.84	−2.39
				3.2–4.8	Peaks 3 and 4	56	−2.50	32	560	30	1220	−2.11	−4.11
				4.8–14	Tail	32	−2.62	33	460	29	1130	−2.34	−4.18
249	910601-69736	2[b]	37	0–23	All[d]	717	−1.88	56	650	81	690	−1.37	−3.43
469	910630-27424	6,[b] 3,[a] 2[a]	76	0–15	All	83	−1.88	91	470	79	540	−1.73	−2.21
503	910709-41604	2,[b] 0,[a] 6[b]	78	0–3	All	107	−1.36	97	2590	88	510	−0.68	−1.79
543	910717-16386	4,[a] 0,[b] 5[b]	81	0–10	All	113	−1.95	121	360	107	360	−1.74	−2.27
676	910814-40182	2,[c] 3[b]	61	0–78	All	204	−1.83	75	480	74	400	−1.40	−2.62
				40–54	Peak 1	152	−1.81	85	520	78	300[c]	−1.23	−2.24
				54–68	Peak 2	184	−1.79	50	600	58	490	−1.30	−2.76
678	910814-69275	2[b]	37	0–69	All	562	−1.51	80	2180	60	1070	−1.00	−2.57
				0–4	Peak	979	−1.46	316	3320	47	1620	−0.72	−3.13
				0–1.7	Rise	435	−1.42	186	3420	39	1400	−0.57	−2.94
				1.7–4	Initial fall	532	−1.45	173	3290	50	1640	−0.75	−3.10
				4–69	Tail	209	−1.61	58	1270	55	640	−1.06	−2.44
841	910930-42931	0,[b] 1[b]	48	0–20	All	74	−1.73	107	550	59	310	−2.28	−1.29
907	911016-39696	2[a]	30	0–102	All[d]	35	−1.11	35	31600	33	580	−3.58	−0.95
1121	911126-46129	5[b]	36	0–60	All	51	−1.83	145	520	51	1720	−1.82	−1.88
				18–30	Peak 1	49	−1.90	102	480	46	2370	−1.87	−2.30
				51–60	Peak 2	33	−2.03	28	380	22	1460	−1.90	−6[c]
1122	911127-15730	5[b]	36	0–28	All	29	−2.29	55	230	28	3230	−2.30	−1.54
				0–10	Rise	27	−2.28	38	250	24	1860	−2.22	−6[c]
				14–28	Tail	34	−2.15	38	230	32	940	−2.37	−1.32
1141	911202-73731	5[a]	30	0–25	All	26	−2.12	28	820	20	700	−1.69	−2.34
				0–6	Peak 1	38	−2.21	25	880	24	1200	−1.77	−3.12
				6–25	Peak 2	19	−2.08	26	760	18	3140	−2.15	−1.66
				10.5–25	Tail	19	−2.13	20	610	18	2060	−2.29	−1.57
1157	911209-66959	5[b]	36	0–25	All	40	−2.01	69	335	39	1120	−2.04	−1.81
				9–16	Peaks 1 and 2	55	−2.12	56	320	50	1530	−2.03	−6[c]
				20–23	Peak 3	32	−2.19	34	280	32	2090	−2.19	−2.04
1235	911227-03955	2[a]	30	0–20	All	31	−2.09	30	710	30	1430	−1.90	−3.62
1288	920110-33480	6[b]	26	0–71	All	33	−1.65	279	890	33	2410	−1.66	−1.47
				0–30	Peak 1	33	−1.69	111	790	31	1880	−1.66	−2.14
				57–68	Big peak	12	−1.76	74	610	12	2270	−1.75	−1.89

[a] The minimum fit energy is 300 keV.
[b] The minimum fit energy is 100 keV.
[c] The fit value tried to exceed the given constraint.
[d] The spectrum contains all available burst-type data, even though some portion of the burst extends beyond the available time interval.

4. DISCUSSION

The statistics of the fraction of bursts showing breaks is subject to several biases. The bursts were selected for their brightness at around 1 MeV, so that soft and weak bursts are underrepresented in the sample tested. Also, the flux at high energies from weak bursts will have large uncertainties, so that spectral breaks that may exist will not be significantly identified. This second bias is emphasized by the fact that the best examples of spectral breaks (in bursts 910814-69275 and 910503-25454) are two of the three highest fluence bursts searched.

Several of the burst spectra have significant curvature, and in two cases this curvature is poorly fitted with a thermal bremsstrahlung model. However, just the fact that this curvature is well fitted by a broken power law does not imply that this is the actual form of the spectra, since other curving functions might well explain the data. Nevertheless, for these two bursts, the curvature apparently is confined to a relatively small energy range. Perhaps the most accurate statement is that roughly a quarter of the bright BATSE spectra show significant curvature which is fully consistent with a broken power law.

If the spectra are indeed broken power laws, then the break is likely to be caused by some photon degradation process. The three bursts apparently without sharp curvature have breaks ranging from 400 to 690 keV, which suggests that photon-photon opacity is the cause. If so, then strong constraints on the burst compactness and distance can be made. The two bursts with sharp curvature have break energies of roughly 1.2 and 1.6 MeV at peak, which suggests that magnetic opacity is the cause. If so, then this is strong evidence for high magnetic fields in bursters.

The various photon degradation processes will produce spectra that are only approximately in the shape of a broken

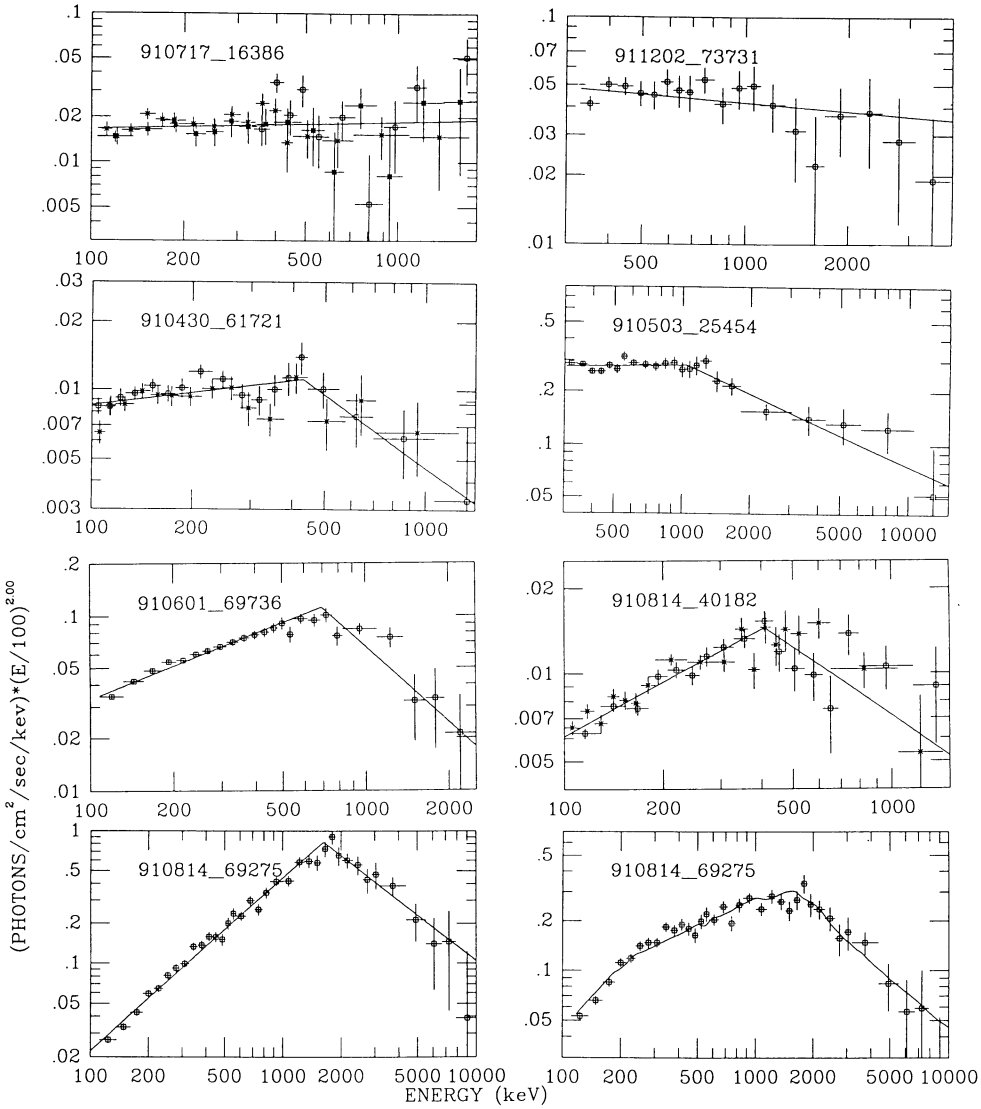

FIG. 1.—Eight BATSE SD spectra. Each panel displays an observed spectrum for a single burst along with a model photon spectrum. The top two panels show photon spectra for which there are no significant high-energy spectral breaks. The four panels in the middle show photon spectra of bursts with significant spectral curvature. The bottom two panels show a photon spectrum (*bottom left*) and a count spectrum (*bottom right*) for the burst with the best defined spectral break. The photon spectra are plotted as $E^2(dN/dE)$, which is the same as νF_ν, so that a flat plot implies equal power emitted per decade of energy. The different symbols are for different detectors, the horizontal error bars indicate the binned channel boundaries, and the vertical error bars indicate the 1 σ uncertainty in the flux. The continuous curve is the best-fit model (either a simple or a broken power law) photon spectrum. In the lower right-hand panel, the curve represents the model count spectrum, that is, it shows the expected count spectrum that would be produced when the model photon spectrum (displayed in the lower left-hand panel) is observed by the BATSE detectors. The small bumps in the model count spectrum are due to small systematic distortions in the detector response matrix and have no significant effect on the model fitting.

power law. Spectral models of general validity are not currently available for these processes. We encourage further theoretical effort toward providing general spectral models that we can fit to the BATSE data.

We thank Teresa Sheets, Anju Basu, Sandhia Mitruka, Nuru Parkar, Phil Brisco, Eswarahalli Panduranga, Elliott Friend, and Martin Brock for the development of the BATSE Spectral Analysis Software.

REFERENCES

Baring, M. G. 1990, MNRAS, 244, 49
Briggs, M. S. 1991, Ph.D. thesis, Univ. California San Diego
Kuznetsov, A. V., et al. 1986, Soviet Astron. Lett., 12, 315
Lampton, M., Margon, B., & Bowyer, S. 1976, ApJ, 208, 177
Loredo, T. J., & Epstein, R. I. 1989, ApJ, 336, 896
Nolan, P. L., Share, G. H., Matz, S., Chupp, E. L., Forrest, D. J., & Rieger, E. 1984, in High Energy Transients in Astrophysics, ed. S. E. Woosley (New York: AIP), 399
Schaefer, B. E. 1991, BATSE Spectral Analysis Software User's Guide (Greenbelt: NASA)
Schaefer, B. E., et al. 1991, Compton Observatory Science Workshop, ed. C. Shrader, B. Dennis, & N. Gehrels (NASA CP 3137)
Schmidt, W. K. H. 1978, Nature, 271, 525
Share, G. H., et al. 1982, in Gamma Ray Transients and Related Astrophysical Phenomena, ed. R. E. Lingenfelter, H. S. Hudson, & D. M. Worrall (New York: AIP), 45
Share, G. H., Matz, S. M., Messina, D. C., Nolan, P. L., Chupp, E. L., Forrest, D. J., & Coopers, J. F. 1986, Adv. Space Res., 6, 15
Zdziarski, A. A. 1987, in 13th Texas Symposium on Relativistic Astrophysics, ed. M. P. Ulmer (Singapore: World Scientific), 553
Zdziarski, A. A., & Lamb, D. Q. 1986, ApJ, 309, L79